

REFINEMENT OF THE STOCHASTIC MODEL OF GOCE SCIENTIFIC DATA IN A LONG TIME SERIES

I. Krasbutter¹, J.M. Brockmann¹, B. Kargoll¹, W.-D. Schuh¹, H. Goiginger², and R. Pail³

¹*Institute of Geodesy and Geoinformation, University of Bonn, 53115 Bonn, Germany, krasbutter@igg.uni-bonn.de*

²*Institute of Navigation and Satellite Geodesy, Graz University of Technology, 8010 Graz, Austria*

³*Institute for Astronomical and Physical Geodesy, TU München, 80290 Munich, Germany*

ABSTRACT

GOCE satellite gravity gradiometry (SGG) data are strongly autocorrelated within the various tensor components (of which we use V_{xx} , V_{yy} and V_{zz}). In order to determine and refine the stochastic model necessary for the determination of the gravity field parameters from these data, we use the Tuning Machine, developed within the GOCE High-level Processing Facility (GOCE-HPF). This tool is based on the method of preconditioned conjugate gradient multiple adjustment (PCGMA), by which the data is processed sequentially on a parallel computer system and in situ via development of the functionals at the actual location and orientation of the gradiometer. The Tuning Machine then allows for an iterative adjustment of the unknown stochastic model in terms of decorrelation filters, which constitute a cascade of autoregressive moving average (ARMA) models.

In this contribution we will present the estimated stochastic model used in the so called time-wise (TIM) GOCE-only gravity field solution. Temporal changes in the stochastic behavior of GOCE measurements are investigated. This data-adaptive stochastic modeling results in a meaningful variance/covariance matrix of the TIM model, as demonstrated e.g. by its application in the combined gravity field GOCO01S and a maximal exploitation of the GOCE signal outside the measurement bandwidth.

Key words: GOCE · Gravity Field Model · Data Decorrelation · ARMA Filter · Temporal Changes.

1. INTRODUCTION

The Tuning Machine, as part of ESA's High-Level Processing Facility (HPF), was designed with the purpose of adjusting and fine-tuning the stochastic model of the gravity gradients observed by GOCE's gradiometer and to obtain an independent gravity field solution [cf. 6, 3, 10]. This solution is determined by applying an iterative solver based on the method of preconditioned conjugate gradients [cf. 8, 2] and the corresponding covari-

ance matrix by means of Monte-Carlo methods [cf. 1]. With this model, the final solution based on the time-wise (TIM) approach [cf. 6, 7] is computed by our project partners at the Institute of Theoretical Geodesy and Satellite Geodesy (Graz University of Technology). In the current paper, we will focus on the Tuning Machine and some new results obtained through it.

Section 2 of this paper begins with an analysis of the general stochastic characteristics of the real-data noise in the time and spectral domain, based on six months of GOCE satellite gravity gradiometry (SGG) data. Then, we will show in Sect. 3 how these characteristics are effectively taken into account by setting up a corresponding stochastic model within the Tuning Machine. The main idea behind this approach will be the application of cascades of autoregressive moving average (ARMA) filters to individual data segments. We will also show, how temporal changes of the stochastic characteristics are taken into account by such filters.

2. CHARACTERISTICS OF THE GRADIOMETER NOISE

We analyzed approximately six months of available real GOCE SGG data (November 2009 until July 2010) both in the time and the frequency domain. It is seen in the upper half of Fig. 1 that these data contain gaps. We divided the data into nine uninterrupted segments, each of these indicated by a distinct color in Fig. 1. As we will see in the following, the stochastic model must be evaluated independently for each of these data segments, as their stochastic characteristics change significantly.

More generally, the gradiometer noise is strongly autocorrelated, which can be seen in the power spectral density (PSD) of the gradiometer noise (see the blue curve in Fig. 2 for a display of one of the data segments); although the noise PSD is relatively flat (i.e. nearly white) inside the measurement bandwidth (between 0.005 and 0.1Hz), it displays a strong, inverse proportional frequency dependence and a large number of sharp peaks between 0 and 0.005Hz. It should be mentioned that this general au-

tocorrelation pattern was to be expected in light of case studies carried out prior to GOCE’s launch [see e.g. 9].



Figure 1. Top: Available GOCE data. The different colors represent uninterrupted data segments. Bottom: Sub-segments resulting from the original segments after outlier deletion and used for filter estimation (V_{zz} component shown).

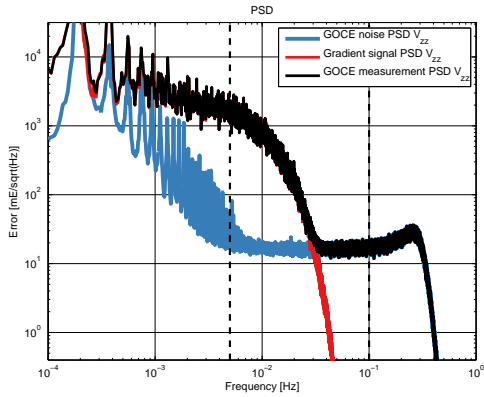


Figure 2. Power spectral density (PSD) of the gradiometer noise for the V_{zz} component, the gradient signal and the measured gravity gradients.

3. MODELING THE GRADIOMETER NOISE

As seen in the previous section the gradiometer noise is strongly autocorrelated. These autocorrelations must be taken into account in the course of the least-squares estimation of the gravity field parameters. A fundamental problem is here that this cannot be accomplished by incorporating these autocorrelations via the data covariance matrix as such a matrix cannot be stored in light of the millions of observations and the resulting memory requirements of more than 20 PetaByte. An effective solution to this problem consists in a full decorrelation (“whitening”) of the gradiometer data by applying a cascade of ARMA filters to the observation equations [cf. 8, 12, 4]. Such a cascade usually consists of different types of ARMA filters by which different aspects of the autocorrelation pattern are modeled and removed from the data. The more accurate a filter describes a certain pattern, the higher is the complexity and number of coefficients of the filter. The effect of filter complexity on the accuracy of the gravity field solution was previously investigated by analyzing two months of GOCE data [cf. 5]. In this section, we will investigate stochastic modeling via decorrelation filtering by analyzing approximately six months of GOCE data.

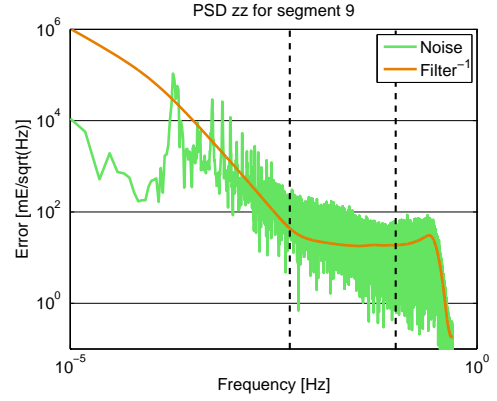


Figure 4. Noise PSD of the unstable segment #9 and inverse PSD of the standard decorrelation filter (# 9024) w.r.t. the V_{zz} component (the other components show a similar behavior).

3.1. Used filter model

An ARMA(p,q) filter is defined by

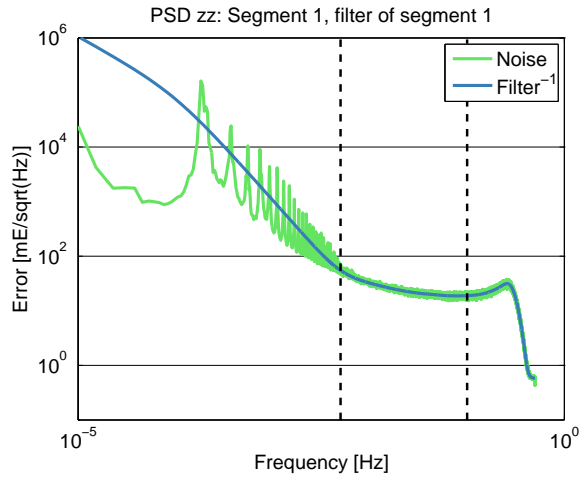
$$y_t = \sum_{k=0}^q \beta_k u_{t-k} + \sum_{k=1}^p \alpha_k y_{t-k}, \quad (1)$$

where u_t, y_t denote the filter input and output, respectively, q, p the orders of the non-recursive and the recursive part of the filter equation, and β_k, α_k the filter coefficients with respect to the non-recursive and the recursive part.

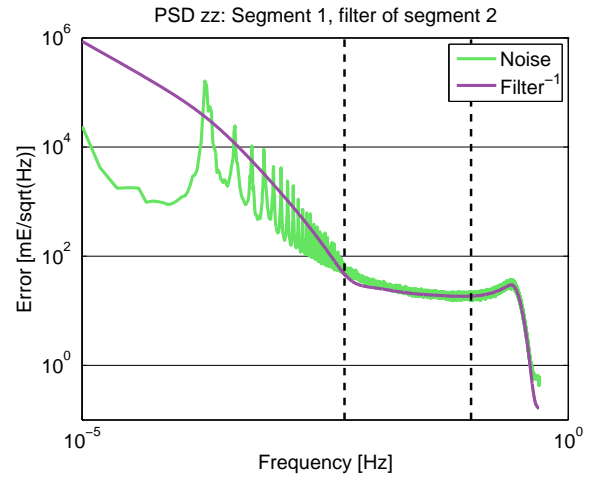
We found it necessary to determine one individual filter cascade per data segment due to the changing stochastic characteristics between segments (see Subsection 3.3). As some of these data segments are very short (see top of Fig. 1 above), the corresponding decorrelation filters may have only a relatively small number of parameters and are not complex in order to minimize further data loss due to filter warm-up. To accomplish this, we used a cascade of one high-pass filter (i.e., a differencing filter with $q = 1, p = 0$ and coefficients $\beta_0 = 1, \beta_1 = -1$) and one ARMA(50,50) filter. We estimated the coefficients of the ARMA(50,50) filter from the high-pass filtered gradiometer noise in a two stage least squares adjustment [see 12, pp 99-100]. It should be mentioned that, due to the restricted filter complexities, we did not add notch filters to the cascade, hence did not model the sharp peaks in the low-frequency part of the noise PSD. It should be mentioned that neglecting the modeling of these peaks does not affect the gravity field solution significantly, however, the corresponding covariance matrix was shown to be less consistent than with notch-filtering of the peaks [5, 11].

3.2. Analysis of stable and instable data segments

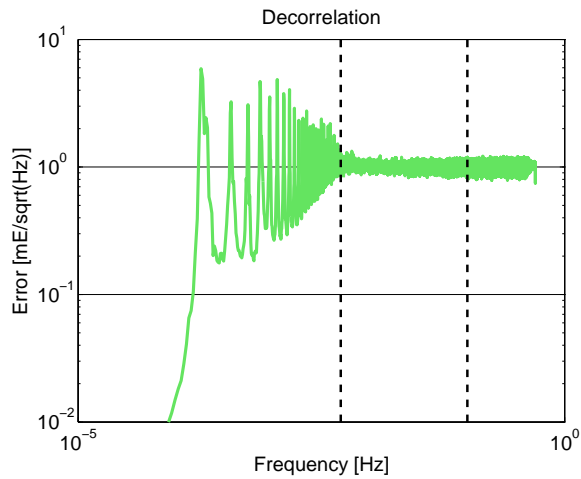
We adjusted the simple decorrelation filter cascade, as explained in the previous subsection, to each of the nine



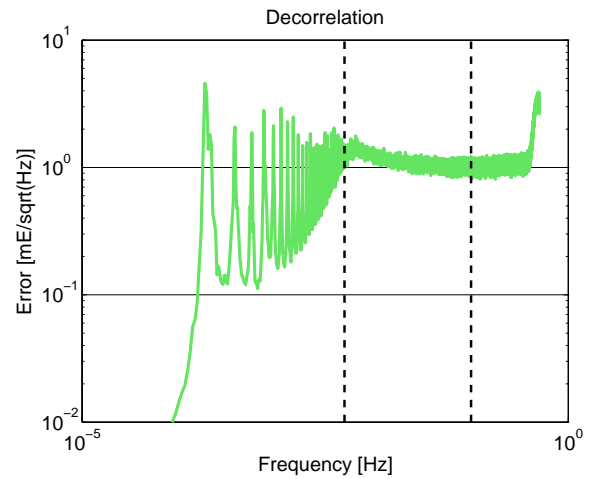
(a) Noise power spectrum of segment #1 and inverse power spectrum of decorrelation filter of segment #1



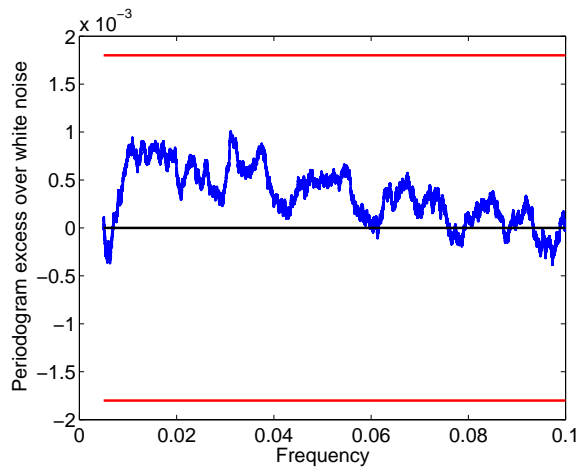
(b) Noise power spectrum of segment #1 and inverse power spectrum of decorrelation filter of segment #2



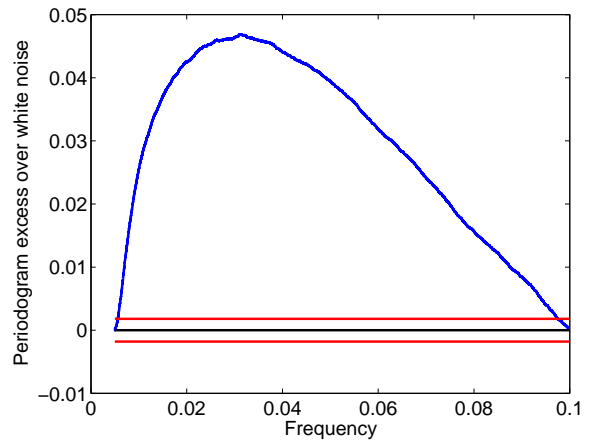
(c) Noise power spectrum after decorrelation with the filter for segment #1



(d) Noise power spectrum after decorrelation with the filter for segment #2



(e) White noise test applied to the measurement bandwidth w.r.t. decorrelated noise as shown in (c)



(f) White noise test applied to the measurement bandwidth of the decorrelated noise as shown in (d)

Figure 3. Left: Decorrelation of data segment #1 with the corresponding filter of this segment. Right: Decorrelation of data segment #1 with the filter of segment #2.

given data segments. Here we encountered, besides the already mentioned data gap problem, the additional difficulty of large numbers of outliers, caused for instance by beam-outs. Due to the strong deteriorating effect of such outliers, we had to restrict the filter estimation to uninterrupted, outlier-free sub-segments of the original nine data segments (see bottom of Fig. 1 above), which we determined through a visual inspection of the data.

We found the filter estimation from segments #3 and #9 to be unstable due to the very large percentage of outliers (100% for segment #3 and 38% for segment #9), i.e., no reasonable filter estimation was possible. The best approach to circumvent this problem was to use a fixed filter (# 9024), as it approximates the stochastic noise characteristics reasonably well (see Fig. 4). This filter was used in the first official GOCE gravity field model of the time-wise approach [11].

The other segments (#1, #2, #4, #5, #6, #7 and #8) were found to be stable, and thus estimation of individual filters was possible. In Fig. 5 the result for segment #1 is shown: the overall fit to the noise characteristics is adequate, but the sharp peaks in the low-frequency part of the spectrum are ignored.

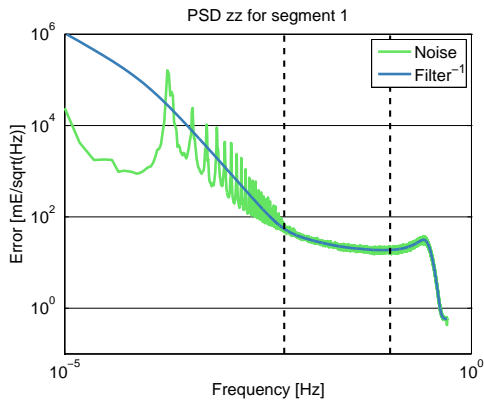


Figure 5. Noise PSD of the stable segment #1 and inverse PSD of the estimated decorrelation filter cascade w.r.t. the V_{zz} component (the other components show a similar behavior).

3.3. Analysis of temporal changes

As mentioned above, we suspected temporal changes of the stochastic properties of the gradiometer noise, requiring the estimation of an individual decorrelation filter cascade for each of the given data segments. In Fig. 6 the spectral behavior of the filter cascade for each of the data segment is shown. Differences between the individual segments are clearly visible, especially around the lower limit of the measurement bandwidth the decorrelation filters have different characteristics.

Another possibility to show that changes between segments necessitate estimation of individual filters for all

segments, is to decorrelate a data segment with the filter of another segment. For reference, Fig. 3(c) shows the result for decorrelation of the first segment with the decorrelation filter of this segment. By contrast, Fig. 3(d) shows the result of the decorrelation of segment #1 with the filter adjusted to segment #2. We see that in particular the decorrelation result is not optimal at the lower limit at the measurement bandwidth when using the filter of another segment. A white noise test (applied to the measurement bandwidth), where the cumulated periodogram of white noise is compared with the cumulated periodogram of the decorrelated gradiometer noise, strongly supports this result. Fig. 3(f) shows a significant difference (blue curve) between white noise and the noise decorrelated by the filter of segment #2. In contrast the difference of the periodograms are marginal and not significant by using the filter of segment #1 (see Fig. 3(e)).

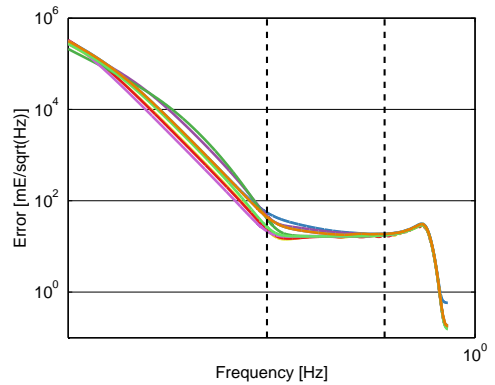


Figure 6. Inverse power spectrum of all decorrelation filters w.r.t. the V_{zz} component.

4. SUMMARY AND CONCLUSIONS

In this paper the available six months of real GOCE SGG data were divided into nine uninterrupted segments. For each segment one individual simple decorrelation filter (which ignores the peaks in the low-frequency part of the noise PSD) was estimated so that the temporal changes of the characteristics of the of the GOCE data are properly taken into account by these filters. For two of the segments the percentage of outliers is very large. Although a filter estimation was not possible in these cases, a prior fixed filter (#9024) could be used as decorrelation filter.

The close fitting of digital decorrelation filter to the stochastic behavior of the GOCE SGG data is not only crucial for the computation of realistic gravity parameters, but also for the derivation of a corresponding realistic full covariance matrix. This covariance matrix is e.g. applied in the combined gravity fields of the GOCO series.

Acknowledgments: Parts of this work were financially supported by the BMBF Geotechnologien program REAL GOCE and the ESA GOCE HPF contract No.

18308/04/NL/MM. The computations were performed on the JUROPA supercomputer in Juelich. The computing time was granted by the John von Neumann Institute for Computing (project HBN15).

REFERENCES

- [1] Alkhatib, H. (2007) On Monte Carlo methods with applications to the current satellite gravity missions. Dissertation, <http://hss.ulb.uni-bonn.de/2007/1078/1078.htm>, Institute of Geodesy and Geoinformation, University of Bonn.
- [2] Boxhammer, C. (2006) Effiziente numerische Verfahren zur sphärischen harmonischen Analyse von Satellitendaten. Dissertation, Institute of Geodesy and Geoinformation, <http://hss.ulb.uni-bonn.de/2006/0799/0799.htm>, University of Bonn.
- [3] Brockmann, J.M., B. Kargoll, I. Krasbutter, W.-D. Schuh and M. Wermuth (2010) GOCE data analysis: from calibrated measurements to the global Earth gravity field. Flechtner, F., T. Gruber, A. Güntner, M. Manda, M. Rothacher, T. Schöne and J. Wickert (eds.), System Earth via Geodetic-Geophysical Space Techniques, Advanced Technologies in Earth Sciences, Springer Berlin, 213-229.
- [4] Krasbutter, I. (2009) Dekorrelation und Daten-TÜV der GOCE-Residuen. Diploma thesis, University of Bonn.
- [5] Krasbutter, I., J. M. Brockmann, B. Kargoll and Schuh W.-D. (2010) Stochastic model refinements for GOCE gradiometry data. In: BMBF: Geotechnologien Science Report No. 17.
- [6] Pail, R., B. Metzler, B. Lackner, T. Preimesberger, E. Höck, W.-D. Schuh, H. Alkathib, C. Boxhammer, C. Siemes and M. Wermuth (2006) GOCE gravity field analysis in the framework of HPF: operational software system and simulation results. In: 3. GOCE user workshop. ESA, Frascati.
- [7] Pail, R., H. Goiginger, R. Mayrhofer W.-D. Schuh, J.M. Brockmann, I. Krasbutter, E. Höck and T. Fecher (2010) Global gravity field model derived from orbit and gradiometry data applying the time-wise method. In: ESA Living Planet Symposium. SP-686, Bergen.
- [8] Schuh, W.-D. (1996) Tailored numerical solution strategies for the global determination of the Earth's gravity field, Vol. 81 Mitteilungen der geodätischen Institute der Technischen Universität Graz. TU Graz.
- [9] Schuh, W.-D., C. Boxhammer and C. Siemes (2006) Correlations, variances, covariances - from GOCE signals to GOCE products. In: 3. GOCE user workshop. ESA, Frascati.
- [10] Schuh, W.-D., J.M. Brockmann, B. Kargoll and I. Krasbutter (2010a) Adaptive optimization of GOCE gravity field modeling. In: Münster, G., D. Wolf and M. Kremer (eds.), NIC Symposium 2010, Vol. 3 IAS Series. Jülich, Germany, 313-320.
- [11] Schuh, W.-D., J.M. Brockmann, I. Krasbutter and R. Pail (2010b) Refinement of the stochastic model of GOCE scientific data and its effect on the in-situ gravity field solution. ESA Living Planet Symposium Bergen, Proceedings, ESA-SP-686.
- [12] Siemes, C. (2008) Digital filtering algorithms for decorrelation within large least squares problems. Dissertation, <http://hss.ulb.uni-bonn.de/2008/1374/1374.htm>, Institute of Geodesy and Geoinformation, University of Bonn.